Fractional Crystallization: Design Alternatives and Tradeoffs

Susan R. Dye and Ka M. Ng
Dept. of Chemical Engineering, University of Massachusetts, Amherst, MA 01003

Guidelines for the design of fractional crystallization processes to separate two- and three-solute mixtures are presented. By using solvent addition/removal, stream combination, and cooling/heating, these processes bypass regions of multiple saturation in the phase diagram and recover pure solutes. Design equations are formulated, and the constraints on the design variables are identified. Also included is a discussion of the effect on recycle flows of changes in the design variables and an estimate of the cost of a fractional crystallization separation.

Introduction

Crystallization plays a significant role in the separation and purification of many organic and inorganic materials (Rousseau, 1987; Myerson, 1993; Mullin, 1993). Like distillation, it yields a pure product, rather than transferring the product from one phase to another as in extraction and absorption. However, compared to the voluminous literature on multicomponent distillation process design (Nishida et al., 1981), relatively little is available on multicomponent crystallization (Dye et al., 1995). This is a serious omission because multicomponent mixtures are prevalent in the chemical processing industry. A well-known example is the separation of a mixture of para- and meta-xylenes. Another example is the production of adipic acid, during which significant amounts of glutaric and succinic acids are produced as byproducts (Sciance and Scott, 1967). Yet another example is the production of potash from sylvinite, which is a mixture of solids consisting primarily of potassium chloride and sodium chloride (Rajagopal et al., 1988; Ng, 1991). With the increasing emphasis on the manufacture of specialty chemicals consisting of complex molecules, crystallization is bound to receive the attention it deserves in the process design community.

Fractional crystallization recovers pure solutes from a multicomponent solution using operations such as heating/cooling, solvent addition, and solvent removal. The fractional crystallization flowsheet employs evaporative crystallizers, thereby restricting the process compositions to isothermal slices of the phase diagram. This distiguishes it from extractive crystallization, a multicomponent separation process in which only cooling crystallization is used (Dale, 1981; Rajagopal et al., 1991; Dye and Ng, 1995). It should be noted that since there is a significant overlap between the applicability of many crystallization terms, fractional crystallization is often considered synonymous with melt crystallization, in which a melt is purified without the presence of a solvent (Fischer et al., 1984; Gilbert, 1991); however, melt crystallization is not discussed in this article.

Of the limited publications on fractional crystallization design, Fitch (1970) provides one of the most comprehensive discussions. His review covers the basic operations to effect separation, such as heating/cooling. It also discusses various phase behaviors such as that for systems with hydrate or compound formation, that solutions of salts with a common ion, and that for systems of conjugate salts. Cisternas and Rudd (1993) developed material balances for the separation techniques discussed in Fitch. This is important because the costs for the plant are directly related to the flow rates in the process.

These previous designs, however, are based on multiple saturation points at which cocrystallization of two or more compounds occurs. While this simplifies the design procedure, it is inadvisable because the avoidance of cocrystallization is absolutely critical in practice in order to produce pure products. For this reason, we provide in this article designs that do not invoke this simplifying assumption. In addition, new process alternatives, operability issues, and costs are considered. We focus on the separation of binary and ternary mixtures that do not form hydrates or compounds.

Phase Behavior

We begin with the isothermal phase behavior of a mixture

Correspondence concerning this article should be addressed to K. M. Ng.

of two solutes (A, B) and a solvent (S), which can be reported as weight fraction on a triangular phase diagram (Figure 1a). Each vertex of the ternary diagram is labeled with a boldface letter, **A**, **B**, or **S**, while A (B) denotes a point along the melting curve for component A (B) at the given temperature. The *single-saturation curve* (dashed line) serves as a boundary between a region of homogeneous unsaturated solutions and a region where precipitation occurs; along the curve the solution is saturated with one of the solutes. A solution with a composition in region **A**-A-AB precipitates A because it contains A in a concentration above the possible saturation concentrations of the line A-AB. In region **B**-B-AB, the compositions are those at which a solution precipitates B. At point A (B), a solution is saturated with A (B). At AB, on the other hand, the solution is saturated with both A and B. This composition is referred to as the *double-saturation point*. The saturation curve of Figure 1a and a second saturation curve are both shown in the temperature-composition phase diagram of Figure 1b. This second saturation curve is for a colder temperature T_c (solid line), while the first is for a higher temperature, T_h (dashed line).

If three of the two-solute, isothermal phase diagrams, such as that shown in Figure 1a, are assembled as shown in Figure 2a, the phase behavior representation can be extended to three solutes and a solvent. The three faces of the tetrahedron that involve equilibria between two solutes and the solvent have a double saturation point, either AB_h, AC_h, or BC_h. As in Figure 1b, the subscripts h indicate that these compositions correspond to a temperature T_h. These double saturation points are connected by *double-saturation troughs* to the *triple-saturation point* ABC_h, which lies in the interior of the tetrahedron and is the composition at which each of the three solutes has reached the limit of its solubility. Three *single-saturation surfaces* are formed inside the tetrahedron. These three-dimensional surfaces are analogous to the two-dimensional single-saturation curves in Figure 1a, and they represent the locus of compositions at which a solution is saturated in one component. For example, a liquid with a composition located on surface A is saturated with A.

The three-dimensional phase relationships are more conveniently displayed on a two-dimensional Jänecke projection. It is obtained by projecting the surfaces onto the base of the tetrahedron as viewed through the apex of the tetrahedron, **S**. A Jänecke projection has been created in Figure 2a, where the dashed lines on the base are the projections of the double saturation troughs and are the divisions between the triangle's three regions, each of which corresponds to one of the single-saturation surfaces.

Figure 2b, like Figure 2a, depicts the three single-saturation surfaces at T_h; however, it also outlines a prism. A solution whose composition lies within this prism contains B in a concentration above any of the saturation values represented by surface B. Thus, B would precipitate from such a solution. There are two other such prisms— one for A and the other for C. A solution with a composition that lies below all three of these prisms contains all three solutes above their respective saturation concentrations and precipitates all three solutes. On the other hand, a solution with a composition that lies above the prisms and above the saturation surfaces is unsaturated.

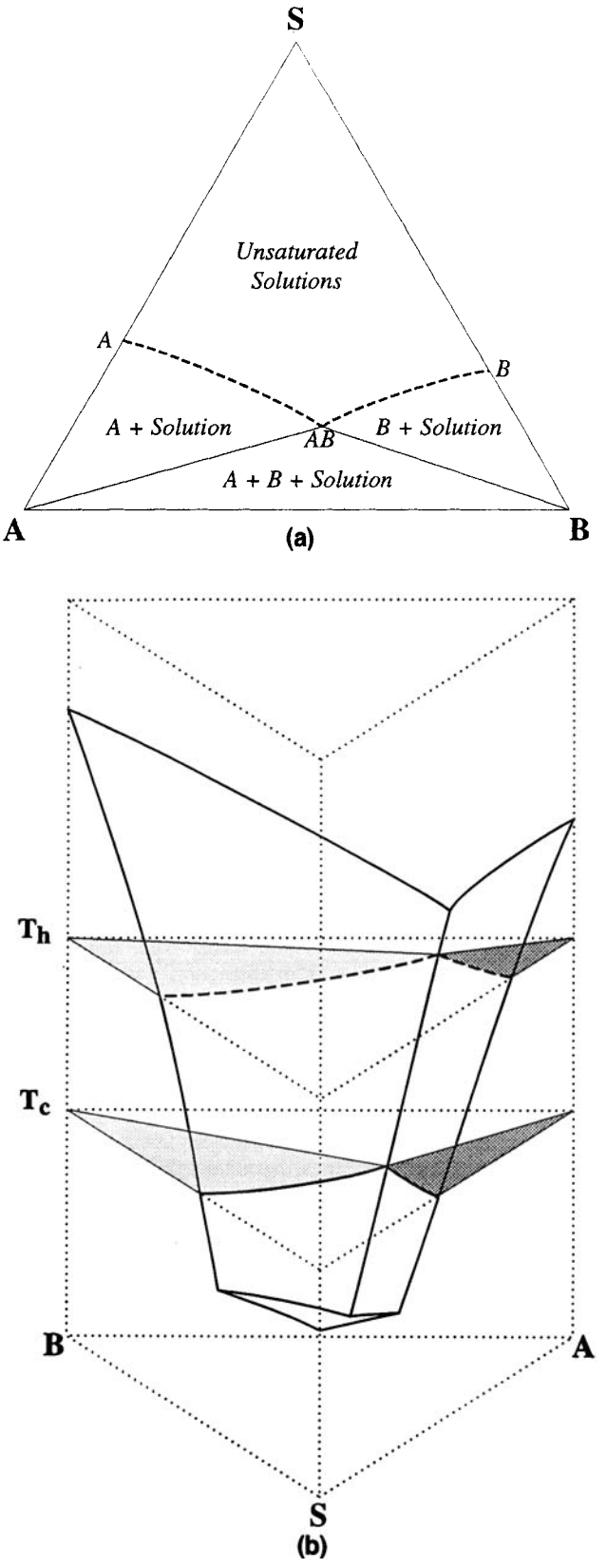

Figure 1. (a)Isothermal solid–liquid triangular phase diagram for a simple-eutectic, two-solute system; (b) isothermal crosssections at T_h and T_c as seen in a temperature-composition diagram.

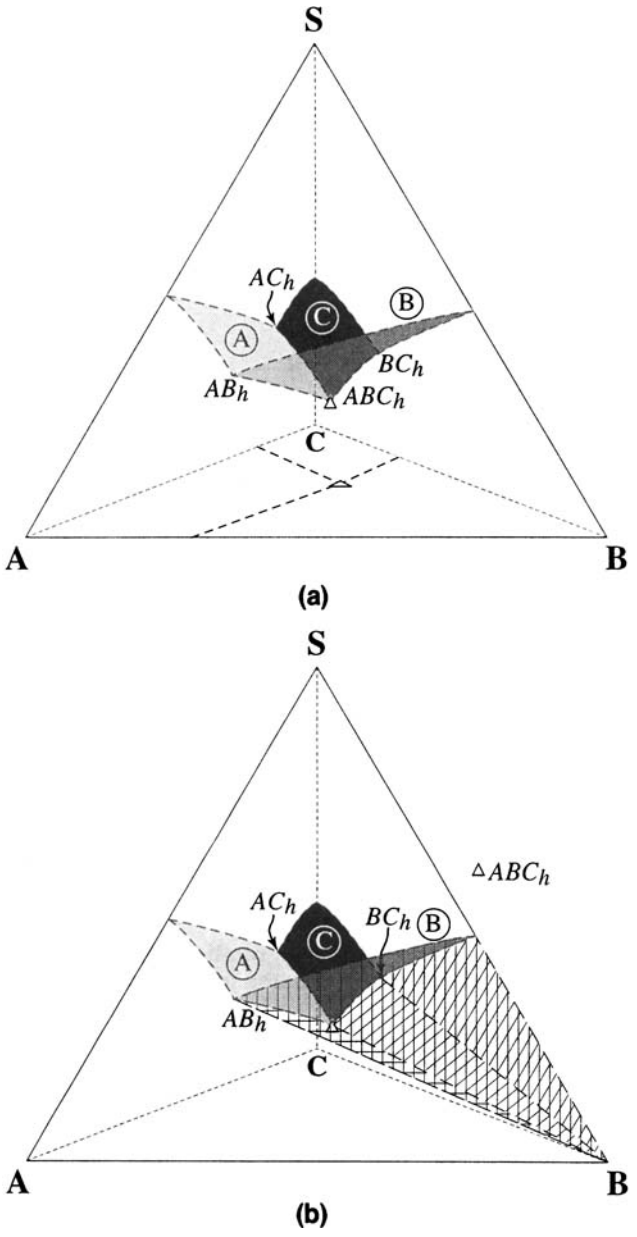

Figure 2. (a)Isothermal tetrahedral phase diagram for a simple-eutectic, three-solute system; (b) prism of single saturation for *B*.

Operations for Effecting Separations

In order to effect a complete separation of a two- or three-solute system, the separation process must precipitate each of the solutes in pure form. This necessitates that the separation process have at least one process composition in each of the regions corresponding to the precipitation of a single solute. Four operations enable a separation process to move from one region to another. They are discussed below for a three-solute system but are equally applicable to two-solute mixtures.

The first operation, *isothermal evaporation*, is illustrated in Figure 3. Solvent is removed from a solution and its composition moves from composition 1 to composition 2, which lies

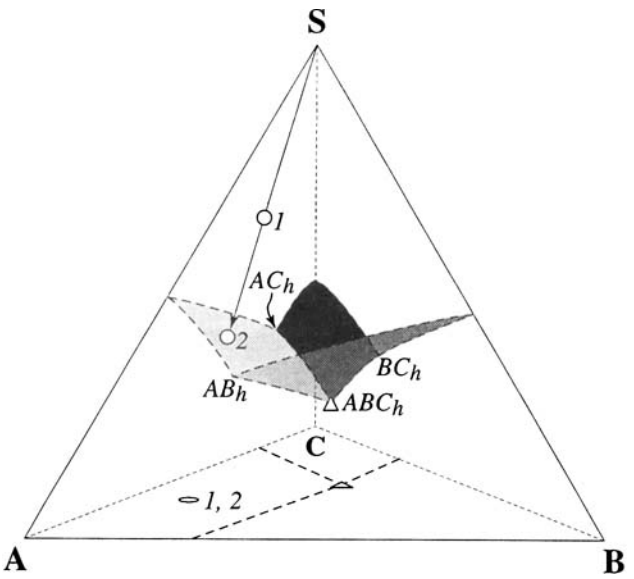

Figure 3. Effect of isothermal evaporation.

on surface A. If solvent removal were continued, crystallization of A would commence. Note that on the Jänecke projection, 1 and 2 appear to be in the same location from the point of view of the solvent. A second operation, *solvent addition*, is simply the reverse of evaporation. The primary purpose of the first two operations is either to create conditions of saturation, or to avoid saturation, respectively. The third operation, pictured in Figure 4, is *stream combination*. Stream 3 is combined with composition 1, the projection of which is in region A, to create composition 2, the projection of which is in region B. The final operation is *heating/cooling*. Figure 5 depicts saturation surfaces for two temperatures, with T_h (dashed lines) higher than T_c (solid lines). Composition 1, which is above saturation surface A at T_h, is a homogeneous liquid. If it is cooled to T_c, A crystallizes. The new liquid composition, 2, is on surface A at the cold temperature. The

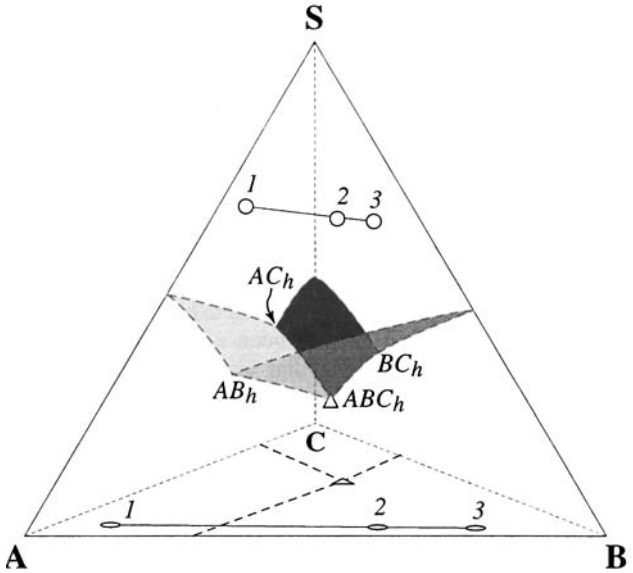

Figure 4. Effect of stream combination.

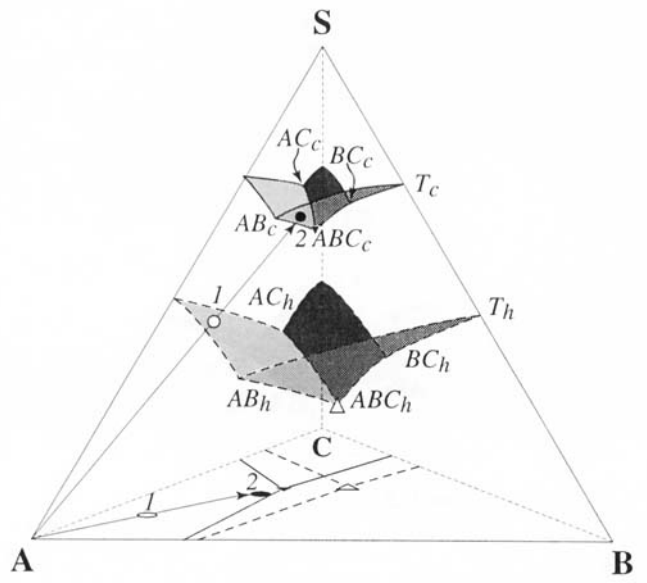

Figure 5. Effect of cooling

Jänecke projection reveals that the projection of composition 1 is in region A at T_h and the projection of composition 2 is in region A at T_c.

Separation of a Two-Solute Mixture

The four operations just described, isothermal evaporation, solvent addition, stream combination, and heating/cooling can be combined to form fractional crystallization flowsheets for both two- and three-solute systems. Guidelines for generating these flowsheets are discussed below.

Each of the two-solute separation processes begins by subjecting the feed to one or more of the four operations so that only one of the two solutes exceeds its solubility limit. After a quantity of this solute is filtered and removed, the operations are used once again to force the other solute to exceed its solubility limit. The configuration of the flowsheet depends on the phase behavior as well as the composition of the feed. This design procedure is illustrated with an example with two solutes below.

A/B separation

Figure 6a shows a flowsheet that recovers A first and then B and uses two crystallizers at two different operating temperatures; the corresponding process paths are depicted in Figure 6b, where the composition numbers on the phase diagram correspond to the stream numbers on the flowsheet. The compositions that are represented by blackened circles are those of streams that have been cooled to T_c; the open circles are used for streams that are held at temperatures higher than T_c. It should be noted that some features of the phase diagrams are exaggerated in order to allow the composition changes to be marked clearly.

To initiate this process, recycled solutes and solvent in stream 3 are combined with the feed (F), which is assumed to be at temperature, T_h. The composition of the resulting stream, 1, lies on a tie line between 3 and F. Stream 1 is then cooled to temperature T_c while solvent is removed from it.

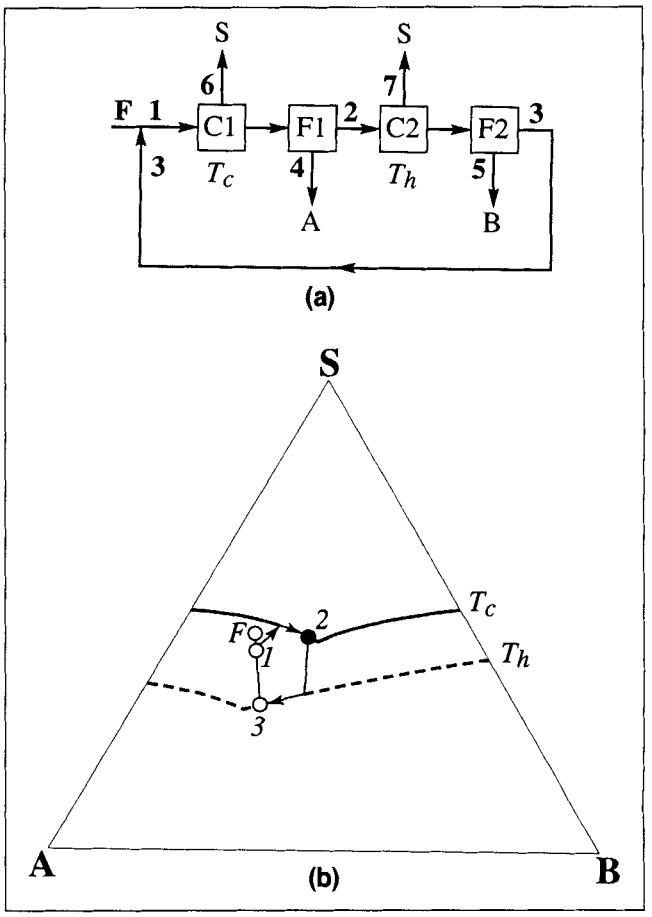

Figure 6. (a) Equipment configuration for *A/B* separation; (b) process paths in the phase diagram.

Although these two operations are carried out simultaneously in crystallizer 1, the effects can be viewed separately. On cooling, the composition of the liquid solution moves on a straight line away from **A**; on evaporation, it moves on a straight line away from **S**. The coupled effect of cooling and evaporation causes the composition to follow the single-saturation curve to composition 2 and to produce crystals of A, which are removed as stream 4. In the next step, the solution is heated back to T_h while more solvent is evaporated. Crystallization of B begins to take place when the liquid composition reaches the single-saturation curve for B at T_h. After the B crystals are filtered away in stream 5, the remaining solutes and solvent are recycled as stream 3. Note that compositions 2 and 3 stop short of their respective double-saturation points. The closer compositions 2 and 3 are to these double-saturation points; the more likely is cocrystallization.

Use of a dilution tank to avoid cocrystallization

Whenever a stream is cooled to induce crystallization, there exists the possibility of cocrystallization. This situation is shown in Figure 7a. Figure 7a differs from Figure 6b in that the composition of stream 1 lies within the triangular area outlined by dotted lines; in this triangular area two solids are in equilibrium with a liquid. If the equipment configuration of Figure 6a were applied to the phase diagram of Figure 7a,

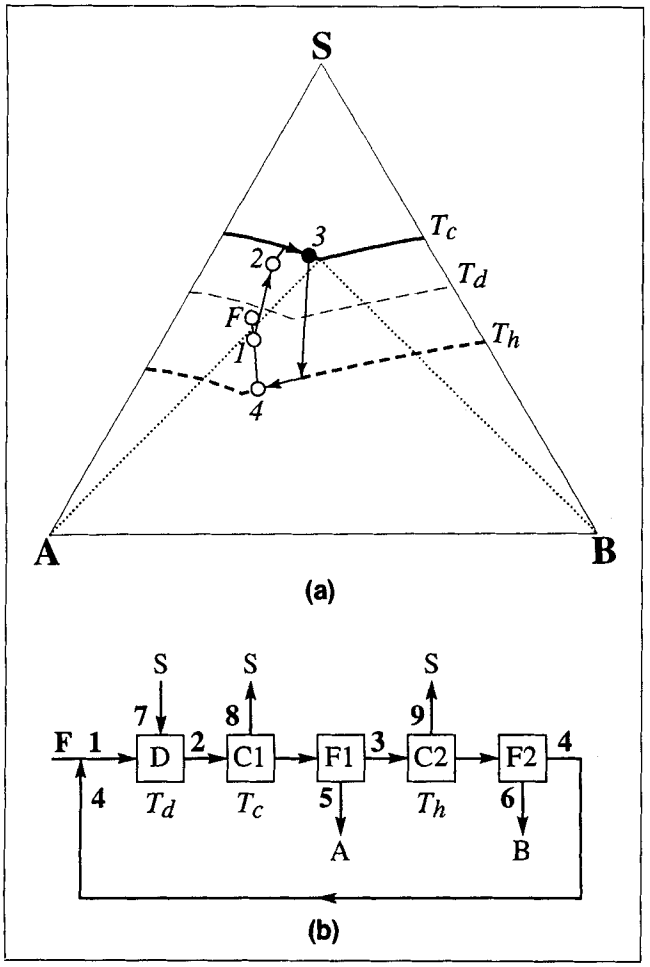

Figure 7. (a) Process paths for the separation with dilution tank; (b) the corresponding equipment configuration.

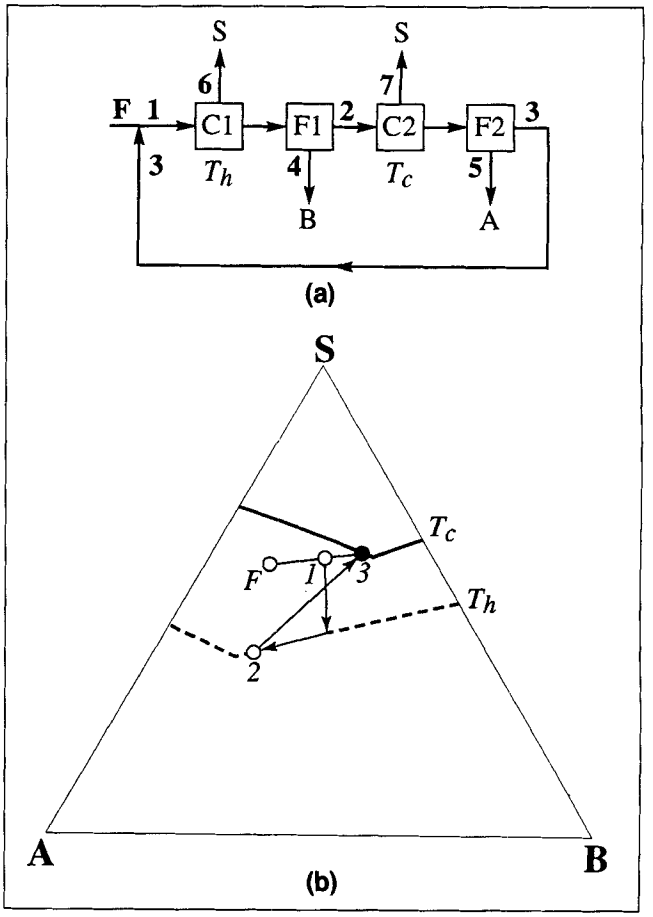

Figure 8. (a) Equipment configuration for *B/A* separation; (b) process paths in the phase diagram.

stream 1 would be cooled to T_c and cocrystallization of A and B would result. To avoid this potential operating problem, the equipment configuration of Figure 7b is used and stream 1 is sent to a dilution tank, where its composition is altered by solvent addition (stream 7). The dilution tank temperature, T_d, should be such that stream 2 is a liquid. The solvent removed from crystallizer 1, stream 8, can be set to zero by adjusting stream 7 such that composition 2 lies on the tie line connecting A and composition 3. One might argue that, provided cooling and solvent addition take place simultaneously in crystallizer 1, any crystals of B formed would redissolve before being removed from the crystallizer and that a dilution tank might not be necessary. However, it is well-known that encrustation of crystal A in crystal B or vice versa often occurs during cocrystallization, a problem that can be prevented simply by the use of a dilution tank.

B/A separation

The equipment configuration shown in Figure 8a and the corresponding phase diagram shown in Figure 8b are for a process that recovers B first and then A. The feed stream F is fed directly into a crystallizer maintained at a temperature T_h. Solvent is evaporated from this crystallizer in stream 6. Crystals of B are removed in stream 4. The effluent mother liquor stream 2 enters crystallizer 2, where it is cooled to T_c, and A is recovered.

A heuristic in process design states that the most plentiful in a multicomponent mixture should be recovered first. As shown in Figures 6a and 8a, this can be achieved by assigning a higher temperature to either crystallizer 1 or crystallizer 2 using the same equipment configuration.

Equipment Configurations for a Three-Solute Mixture

One-loop separations

Separation schemes for three-solute systems, like those for two-solute systems, can be constructed from combinations of the operations described earlier. Figure 9a provides an example equipment configuration of a one-loop separation of three solutes, the first such separation to be disclosed in the literature. The process compositions are marked on both the Jänecke projection (Figure 9b) and the corresponding tetrahedral phase diagram (Figure 9c). In Figure 9b and the figures that follow it, the double saturation troughs for T_h are represented by dashed lines and those for T_c, by solid lines.

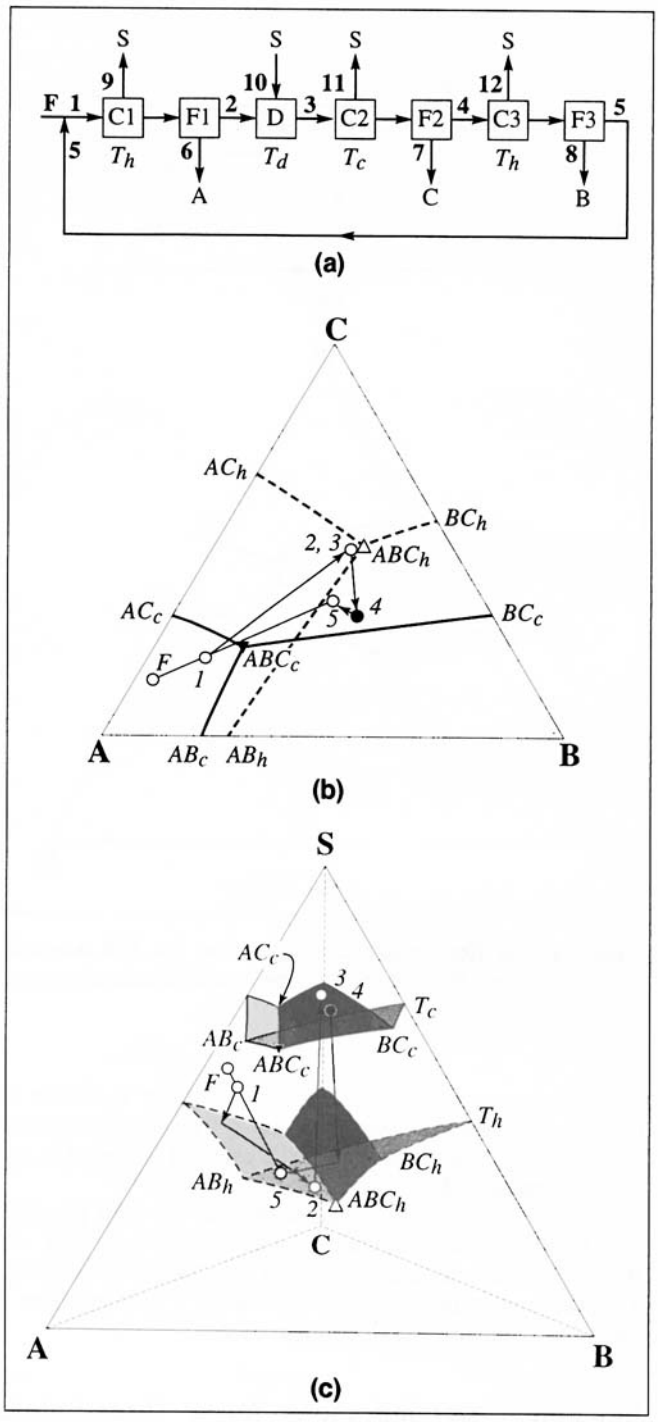

Figure 9. Example one-loop separation of three solutes by fractional crystallization.

(a) Equipment configuration. (b) Projected phase diagram. (c) Example separation of three solutes as it appears on a tetrahedral solid–liquid phase diagram.

Solutes A, B, and C in solvent S are to be separated from each other. The feed, which is assumed to be at T_h, has a composition that lies above the T_h single-saturation surfaces in the tetrahedron. The feed is combined with a recycled solution (stream 5), thereby creating stream 1. Solvent removal from stream 1 causes crystallization of A and the process path follows surface A.

After component A is recovered, the next step is to crystallize pure C. A temperature change can accomplish this objective because region A at T_h overlaps region C at T_c. To avoid potential cocrystallization, stream 2, whose composition lies well below the T_c surfaces, must be subjected to solvent addition in the dilution tank before it undergoes any changes in crystallizer 2. Isothermal evaporation and cooling of the stream that exits the dilution tank lead to the crystallization of only C. If the amount of solvent added to the dilution tank is chosen judiciously, evaporation from crystallizer 2 is unnecessary; that is, stream 11 is nil. In order to recover B, stream 4 is fed to crystallizer 3, which operates at the higher temperature, T_h. Solvent is removed from stream 4 so that the process path moves away from surface C at T_c toward surface B at T_h. Solute B crystallizes as the process path moves along surface B up to composition 5. The effluent mother liquor from crystallizer 3 is recycled in stream 5.

The Jänecke projection of Figure 9b demonstrates three key features of the phase diagram that must be present in order for a clockwise, one-loop separation to succeed when two isotherms are used. That is, recovery of A at one temperature is followed by the recovery of C at the other temperature, and then the recovery of B at the first temperature. First, there must be an overlap between region A at one temperature, say T_h, and the region C at the other, T_c. Similarly, there must be an overlap between region C at that same temperature, T_c, and region B at the other temperature. Secondly, the feed must be in a position such that the removal of A from stream 1 places composition 2 in the area of overlap between region A and region C. Thirdly, the double saturation trough $ABC_h - AB_h$ must not slant in the direction of **B** or even be collinear with the line $\mathbf{C}-ABC_h$. The first and third points are discussed in more detail below.

Two-loop separations

If complete separation cannot be accomplished with the two selected crystallizer temperatures in one loop, it must be carried out in two or more loops. For example, the first condition necessary for the success of a one-loop separation with two isotherms is not satisfied for the phase diagram of Figure 10a. A one-loop separation is impossible because, although region A at T_c overlaps region C at T_h, region C at T_h does not, in turn, overlap region B at T_c. Instead, the separation is accomplished by the equipment configuration pictured in Figure 10b. At the cooler temperature, the feed is combined with stream 5 to create stream 1. Solute A is solidified and removed in the first crystallizer and filter at T_c. In the second crystallizer, A and C are crystallized together at T_c as the process path moves along the double-saturation trough $ABC_c - AC_c$. These two solids from the second crystallizer are sent to a second loop in order to be separated from one another. It is now possible to recover B because stream 3, the effluent from the second crystallizer, has a composition that lies above the B surface of saturation at T_h. Therefore, stream 3 is heated and solvent evaporated from it so that B precipitates. Solvent is added to the effluent from crystallizer 3 in order to avoid cocrystallization when the warm recycle is added to the cold feed.

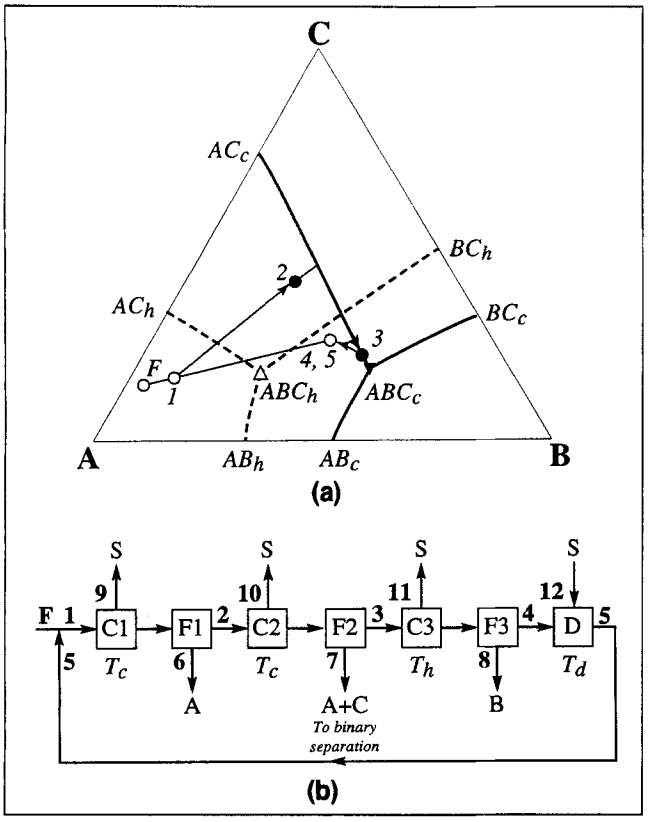

Figure 10. Example two-loop separation of three solutes: (a) projected phase diagram and (b) equipment configuration.

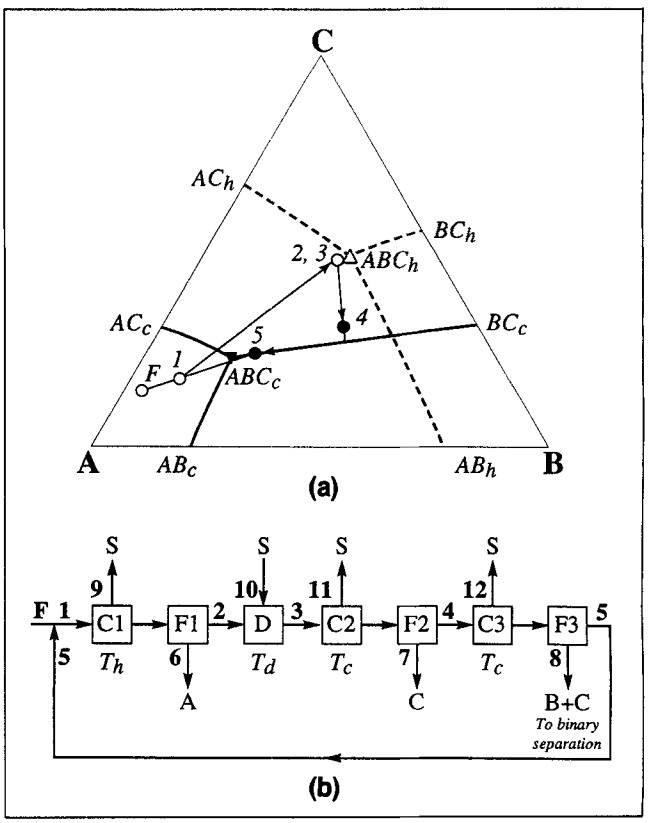

Figure 11. Additional example of a two-loop separation of three solutes.

(a) Projected phase diagram; (b) equipment configuration.

Figure 11a is yet another example of a system that should be separated in two loops. Even though pure A and C are recovered, the slant of the line $ABC_h - AB_h$ precludes recovery of pure B in crystallizer 3. Instead, the equipment configuration of Figure 11b is used; B and C are removed together as a mixture of crystals that can then be separated in another loop by two-solute fractional crystallization, as described previously. Unlike the process of Figure 9a, in which stream 4 is heated while solvent is removed, this process maintains stream 4 at the cooler temperature while the solvent is evaporated. This means that the process path follows surface C at T_c up to and along the double-saturation trough where B and C cocrystallize.

Use of three crystallizer temperatures

There is yet another option overlooked in the literature: the use of more than two isotherms. For example, consider the phase diagram of Figure 12a, which is identical to that of Figure 11a for the T_h and T_c isotherms; complete separation using two isotherms is hampered by the slant of the line $ABC_h - AB_h$. The solutes that form the phase diagram of Figure 12a can be completely separated by the process configuration pictured in Figure 12b. This scheme, unlike that shown in Figure 11b, does not require that the cooling of stream 4 be continued until B and C cocrystallize; instead, stream 4 is heated from T_c to T_i, an intermediate temperature between T_c and T_h. Pure B can be recovered despite the phase behavior at T_h as long as region C at T_c and region B at T_i overlap. In other words, this scheme is independent of the slant of the line $ABC_i - AB_i$.

Design equations for one-loop three-solute separations

For design calculations, it is more convenient to convert the data from the tetrahedral phase diagram to those for a solubility diagram (Figure 13). The single-saturation surfaces are replotted on a set of three perpendicular axes, c_A, c_B, and c_C. Each pair of axes forms a plane that contains two single-saturation curves for a two-solute solution. For example, in the plane formed by c_A and c_B, the joint solubility of A is $S'_A(c_B)$ and that of B, $S'_B(c_A)$. The prime indicates that the solution is saturated with only one component and the symbol in parentheses identifies the concentration on which the solubility depends. The intersection of $S'_A(c_B)$ and $S'_B(c_A)$ is the double-saturation point (S''_A, S''_B)—a solution whose concentrations lie at this point saturated with both A and B. The solubility of a component in a three-solute solution is found on one of the surfaces in three-dimensional space. If component A, for example, is the only solute saturated in a three-solute solution, its joint solubility $S'_A(c_B, c_C)$ is a function of the concentrations of B and C and is found on surface A. The bold curves formed by the intersections of the three single-saturation surfaces are the double-saturation troughs. For example, A and B are saturated along one curve, where their joint solubilities are $S''_A(c_C)$ and $S''_B(c_C)$ and are a

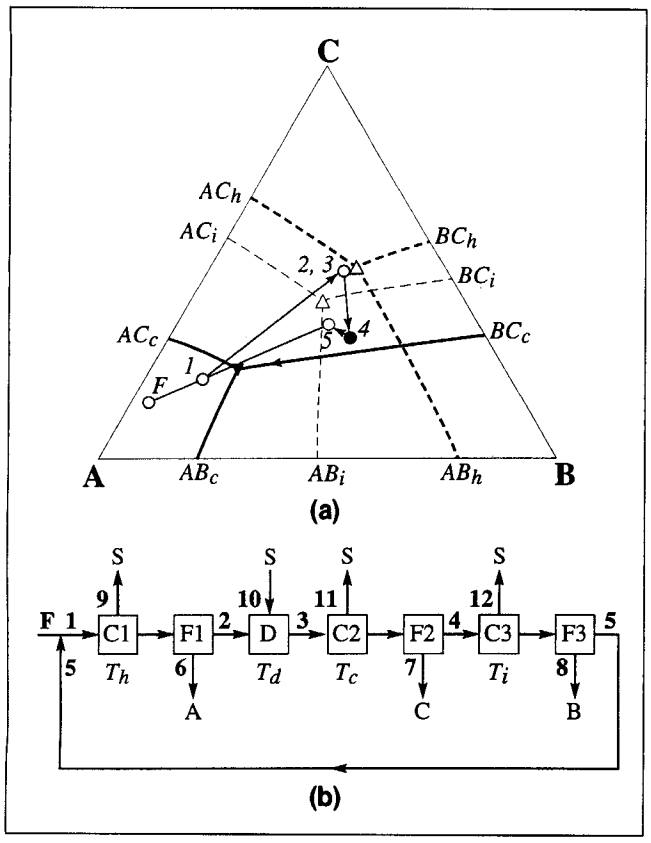

Figure 12. Example one-loop separation of three solutes using three isotherms.

(a) Projected phase diagram; (b) equipment configuration.

function of the concentration of the third solute, C. The intersection of the bold curves is the triple-saturation point, where the joint solubilities are S'''_A, S'''_B, S'''_C.

If a linear relationship is assumed between the solubility of one solute and the concentration of the others, we have

$$S'_A(T, c_B, c_C) = \alpha_1 + \alpha_2 c_B + \alpha_3 c_C \tag{1}$$

$$S'_B(T, c_A, c_C) = \alpha_4 + \alpha_5 c_A + \alpha_6 c_C \tag{2}$$

$$S'_C(T, c_A, c_B) = \alpha_7 + \alpha_8 c_A + \alpha_9 c_B. \tag{3}$$

The solubility behavior of three solutes is completely described by the parameters α_1 through α_9 in Eqs. 1 through 3. Table 1 is a list of the expressions for other joint solubilities. The parameters α_1, α_4, and α_7 can be found by measurement of the pure-component solubility of A, B, and C, respectively; the rest of the parameters can be determined by measurement of the joint solubilities of pairs of solutes at the three double-saturation points followed by the use of the experimentally determined information in Eqs. 10 to 15. Generally, solubility can be correlated by an exponential dependence on temperature; that is, $\alpha_i = \beta_i \exp(\gamma_i T)$ for parameter i. Here, β_i and γ_i are constants.

A few simple material balances characterize the one-loop separation. We begin with the recycle in Figure 9a, stream 5. The flow rate of A in stream 5, $F_A(5)$, is equal to its flow rate in stream 3, since A is neither added nor removed after the first crystallizer. $F_A(5)$ is the concentration of A times the flow rate of solvent, $F_S(3)c_A(3)$. The total amount of solvent in stream 3 is represented by the flow rate of a solute divided by its concentration, such as $[F_{BF} + F_B(5)]/c_B(3)$. Thus, we have

Table 1. Linear Solubility Equations for a Three-Solute Mixture

Single-Saturation Points:			
c_A–c_B plane:	$S'_A(c_B) = \alpha_1 + \alpha_2 c_B$	$S'_B(c_A) = \alpha_4 + \alpha_5 c_A$	(4,5)
c_B–c_C plane:	$S'_B(c_C) = \alpha_4 + \alpha_6 c_C$	$S'_C(c_B) = \alpha_7 + \alpha_9 c_B$	(6,7)
c_A–c_C plane:	$S'_A(c_C) = \alpha_1 + \alpha_3 c_C$	$S'_C(c_A) = \alpha_7 + \alpha_8 c_A$	(8,9)
Double-Saturation Troughs:			
	$S''_A(c_C) = \dfrac{\alpha_1 + \alpha_2\alpha_4 + c_C[\alpha_2\alpha_6 + \alpha_3]}{1 - \alpha_2\alpha_5}$		(10)
	$S''_B(c_C) = \dfrac{\alpha_4 + \alpha_5\alpha_1 + c_C[\alpha_5\alpha_3 + \alpha_6]}{1 - \alpha_2\alpha_5}$		(11)
	$S''_A(c_B) = \dfrac{\alpha_1 + \alpha_3\alpha_7 + c_B[\alpha_3\alpha_9 + \alpha_2]}{1 - \alpha_3\alpha_8}$		(12)
	$S''_C(c_B) = \dfrac{\alpha_7 + \alpha_8\alpha_1 + c_B[\alpha_8\alpha_2 + \alpha_9]}{1 - \alpha_3\alpha_8}$		(13)
	$S''_B(c_A) = \dfrac{\alpha_4 + \alpha_6\alpha_7 + c_A[\alpha_6\alpha_8 + \alpha_5]}{1 - \alpha_6\alpha_9}$		(14)
	$S''_C(c_A) = \dfrac{\alpha_7 + \alpha_9\alpha_4 + c_A[\alpha_9\alpha_5 + \alpha_8]}{1 - \alpha_6\alpha_9}$		(15)
Triple-Saturation Point:			
	$S'''_C = \dfrac{\alpha_7 - \alpha_2\alpha_5\alpha_7 + \alpha_1\alpha_8 + \alpha_2\alpha_4\alpha_8 + \alpha_1\alpha_5\alpha_9 + \alpha_4\alpha_9}{1 - \alpha_2\alpha_5 - \alpha_2\alpha_6\alpha_8 - \alpha_3\alpha_8 - \alpha_3\alpha_5\alpha_9 - \alpha_6\alpha_9}$		(16)
	$S'''_B = \dfrac{\alpha_4 + \alpha_1\alpha_5 + [\alpha_3\alpha_5 + \alpha_6]S'''_C}{1 - \alpha_2\alpha_5}$		(17)
	$S'''_A = \dfrac{\alpha_1 + \alpha_2\alpha_4 + [\alpha_2\alpha_6 + \alpha_3]S'''_C}{1 - \alpha_2\alpha_5}$		(18)

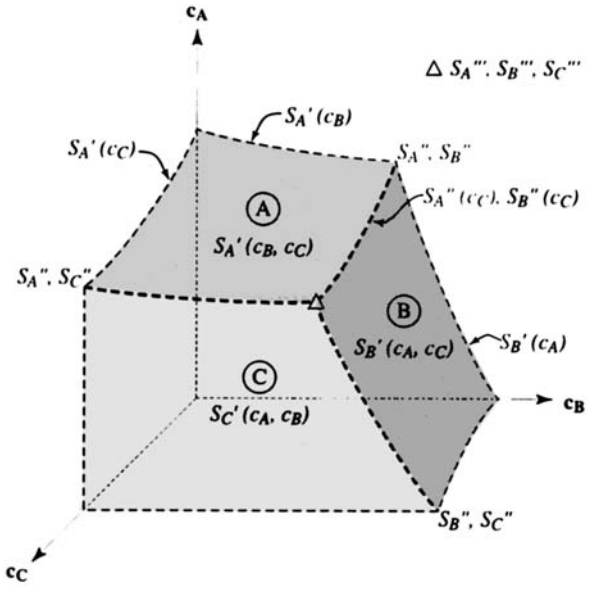

Figure 13. Example solubility surfaces of a three-solute system at T_h.

$$F_A(5) = \frac{F_{BF} + F_B(5)}{c_B(3)} c_A(3). \tag{19}$$

Following this same line of reasoning, we get for the remaining three components

$$F_B(5) = \frac{F_A(5)}{c_A(5)} c_B(5) \tag{20}$$

$$F_C(5) = \frac{F_B(5)}{c_B(5)} c_C(5) \tag{21}$$

$$F_S(5) = \frac{F_B(5)}{c_B(5)} c_S(5) = \frac{F_B(5)}{c_B(5)}. \tag{22}$$

Substitution of Eq. 20 into Eq. 19 gives

$$F_A(5) = \frac{F_{BF}}{\dfrac{c_B(3)}{c_A(3)} - \dfrac{c_B(5)}{c_A(5)}} = \frac{F_{BF}}{R_{BA3} - R_{BA5}}, \tag{23}$$

where R_{BA3} and R_{BA5} are the concentration ratios between B and A in streams 3 and 5, respectively. Substituting Eq. 23 into Eq. 20, we get

$$F_B(5) = \frac{F_{BF}\, R_{BA5}}{R_{BA3} - R_{BA5}}. \tag{24}$$

We also obtain from Eqs. 21 and 22

$$F_C(5) = \frac{F_{BF}}{R_{BA3} - R_{BA5}} \frac{R_{BA5}}{R_{BC5}} \tag{25}$$

$$F_S(5) = \frac{F_{BF}}{R_{BA3} - R_{BA5}} \frac{R_{BA5}}{c_B(5)}. \tag{26}$$

The conditions under which the one-loop separation succeeds were described earlier. However, the material balances reveal one additional restriction: $R_{BA3} > R_{BA5}$. Since stream 5 is saturated with B but unsaturated with A and C, we can use Eq. 2 to calculate $c_B(5)$ in Eq. 26; that is,

$$c_B(5) = \alpha_4 + \alpha_5 c_A(5) + \alpha_6 c_C(5). \tag{27}$$

Rearrangement yields

$$c_B(5) = \left[\frac{1}{\alpha_4} - \left(\frac{\alpha_5}{\alpha_4}\right)\left(\frac{1}{R_{BA5}}\right) - \left(\frac{\alpha_6}{\alpha_4}\right)\left(\frac{1}{R_{BC5}}\right)\right]^{-1}. \tag{28}$$

The design variables are the crystallizer and dilution tank temperatures, T_h, T_d, and T_c, and the mass ratios, R_{BA3}, R_{BA5}, and R_{BC5}. The temperatures determine the phase behavior and solubility surfaces. R_{BA3} restricts the location of composition 3 to a line of constant concentration ratio between A and B. R_{BA5} and R_{BC5} fix the location of composition 5.

The chosen values for the design variables are put into the material balances so that the flow rates of all streams can be determined. The only remaining unknowns are the amounts of solvent that must be evaporated from the crystallizers or fed to the dilution tank. These are calculated with knowledge of the joint solubilities of the solutes. For example, the solvent that must be removed from crystallizer 1 is the difference between the solvent in the feed to the crystallizer and that in the effluent. Since only A is saturated in crystallizer 1, the amount of solvent that leaves the crystallizer in stream 2 is the flow rate of A in stream 2 divided by the saturation concentration of A at the given conditions. Thus, we have

$$F_S(9) = F_S(1) - \frac{F_A(2)}{S'_A(T_h, c_B(2), c_C(2))}$$

$$= F_S(1) - \frac{F_A(2)}{\alpha_1 + \alpha_2\left(\dfrac{F_B(2)}{F_S(2)}\right) + \alpha_3\left(\dfrac{F_C(2)}{F_S(2)}\right)}. \tag{29}$$

Example One-Loop Separation

The following example illustrates the one-loop, three-solute, fractional crystallization scheme. The input parameters are given in Table 2. The tetrahedral phase diagram for this system is plotted in Figure 14a; the Jänecke projection plotted in Figure 14b reveals that a one-loop separation is feasible. This is the phase behavior representative of a system of highly soluble solutes such as an aqueous solution of adipic, glutaric, and succinic acids. Distillation cannot be used for separating this mixture because adipic acid decomposes at its boiling point.

Process sensitivity and geometric constraints

The compositions and flow rates of this one-loop process are calculated according to the method described earlier. In Figures 15, 16, and 17 the parameters R_{BA3}, R_{BA5}, and R_{BC5} are varied. Their effect is assessed by examination of the

Table 2. Values of Input Parameters for the One-Loop Separation

Production Rate (kg/yr)		
A	25.0×10^5	
B	20.8×10^4	
C	14.6×10^5	
S	55.2×10^5	
Feed Composition (mass fraction)		
A	0.258	
B	0.021	
C	0.151	
S	0.570	
Crystallization Temperature (°C)		
T_h	125	
T_c	110	
Heat of Fusion (kJ/kmol)		
A	21,000	
B	35,000	
C	33,000	
S	6,000	
Heat Capacity (J/kg·°C)		
A	1,130	
B	1,297	
C	1,088	
S	4,184	
Solubility Equations		
$S'_A(T_c,c_B,c_C)=0.43+0.36c_B-0.21c_C$		
$S'_B(T_c,c_A,c_C)=0.49-0.90c_A-0.018c_C$		
$S'_C(T_c,c_A,c_B)=0.59-0.78c_A-0.95c_B$		
$S'_A(T_h,c_B,c_C)=0.67+0.042c_B-0.49c_C$		
$S'_B(T_h,c_A,c_C)=0.75-0.64c_A-0.30c_C$		
$S'_C(T_h,c_A,c_B)=0.82+0.37c_A-0.72c_B$		
Saturation Mass Fraction	T_h	T_c
Single		
A	0.400	0.300
B	0.430	0.330
C	0.450	0.370
Double		
A and *B*	0.340, 0.160	0.297, 0.053
A and *C*	0.106, 0.424	0.220, 0.180
B and *C*	0.325, 0.175	0.304, 0.076
Triple		
A, *B* and *C*	0.141, 0.139, 0.298	0.257, 0.059, 0.091

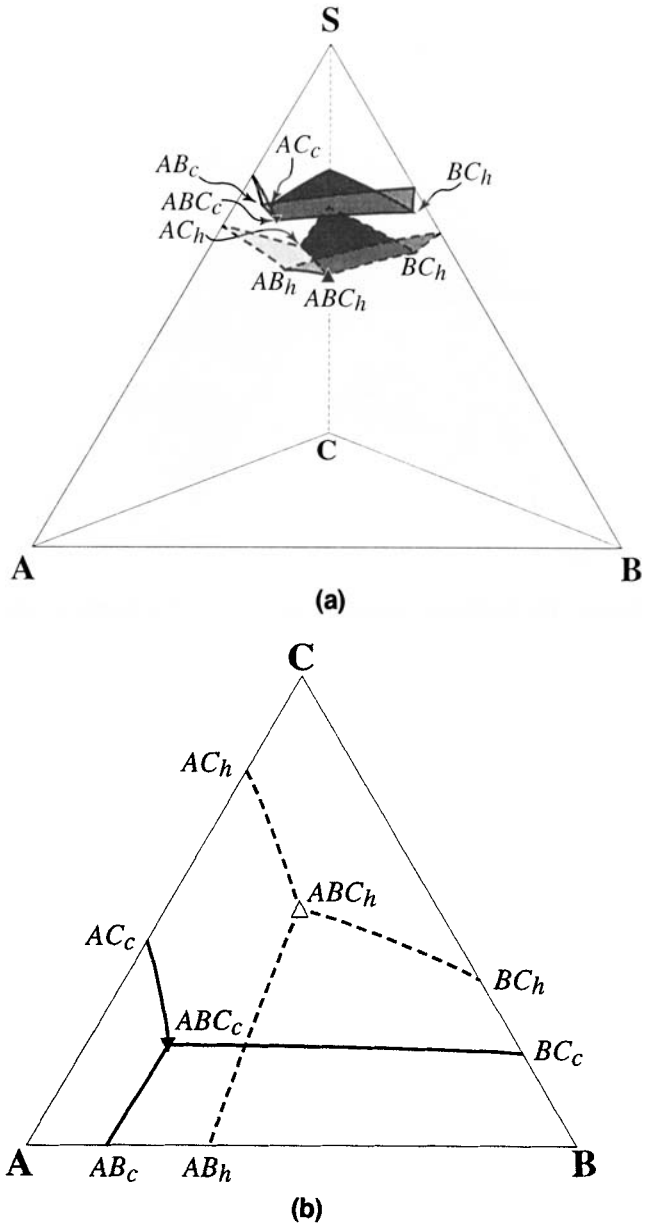

Figure 14. (a)Solid–liquid, tetrahedral phase diagram for a system with the input parameters given in Table 2; (b) Jänecke projection of Figure 14a.

changes in the ratios R_{RF}, R_{S9F}, R_{S10F}, and R_{S12F}—the ratio of the flow rates of streams 5, 9, 10, and 12 to the flow rate of the feed, respectively. The base case values of the design variables are $R_{BA3}=0.88$, $R_{BA5}=0.63$, and $R_{BC5}=1.16$.

The ratio R_{BA3} appears in the denominator of the recycle equations, Eqs. 23 through 26. As it is decreased, the recycle increases, as shown in Figure 15. The solvent flows 9, 10, and 12 also increase with decreasing R_{BA3}, but not as severely as the recycle increases. Increases in R_{BA3} move the projection of process composition 2 slightly toward **B** and more drastically toward **C** (see Figure 9b). This means that increases in R_{BA3} eventually cause stream 2 to be saturated in both *A* and *C*. On the other hand, decreases in R_{BA3} move composition 2 away from **B** and **C** and toward the *AB* double saturation trough. Therefore, there are upper and lower limits for R_{BA3} beyond which multiple saturation occurs.

In Figure 16, the ratio R_{BA5} is increased from its base case value of 0.63. This brings about increases in R_{S9F}, R_{S10F}, R_{S12F}, and R_{RF}. Since the magnitude of the flow of stream 5 increases with increasing R_{BA5}, composition 1 moves closer to composition 5. Furthermore, composition 5 moves toward the *BC* edge of the phase diagram. Both of these change the position of composition 2. Beyond $R_{BA5}=0.72$, stream 2 is multiply saturated in *A* and *B*. Similarly, R_{BA5} cannot be lowered below 0.63 because, even though stream 5 is still on surface *B*, stream 2 becomes saturated in both *A* and *C*.

Figure 17 reveals that the ratio R_{BC5} has little effect on the size of the process streams. If R_{BC5} is increased, composition 5 moves slightly toward the *AB* edge of the phase diagram and toward **A**. Above $R_{BC5}=1.21$, stream 4 is forced into the *BC* double-saturation trough at T_c. Decreases in R_{BC5} move composition 5 slightly toward **C** and away from **A**.

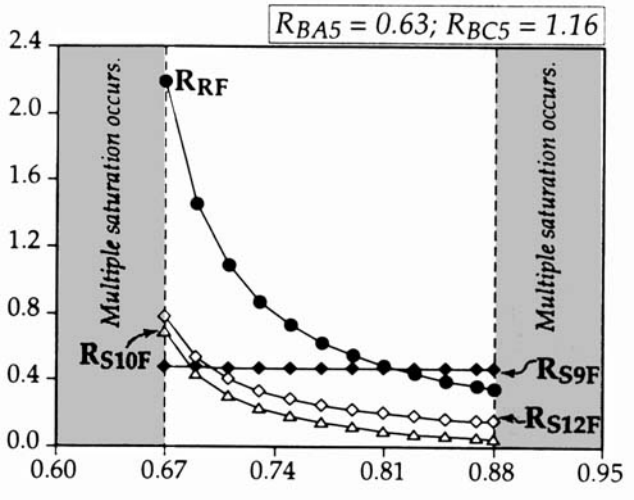

Figure 15. Effect of changes in the ratio R_{BA3}.

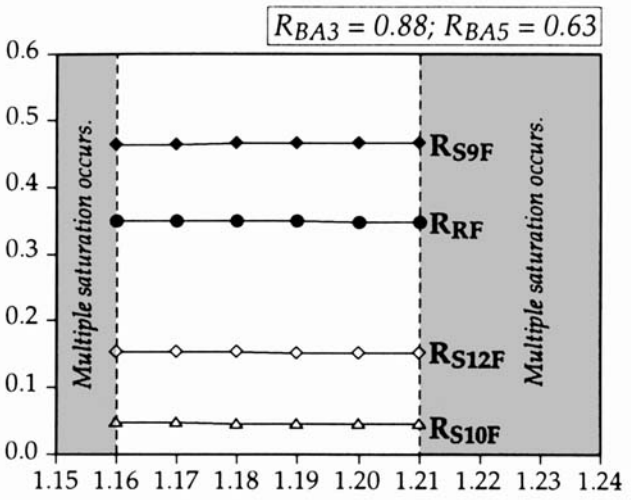

Figure 17. Effect of changes in the ratio R_{BC5}.

When R_{BC5} is below 1.16, because of the material balance relationship between the compositions, stream 2 becomes doubly saturated before stream 5 does.

Capital and operating costs for fractional crystallization

The total annual cost of this separation is estimated to be 510,000 1994 dollars. A capital charge factor of 1/3 is applied to the capital cost, which comprises the annual expenditures for crystallizer tanks, heat exchangers, and filters. The primary operating cost is that of the steam used to vaporize the solvent. The relative contributions of these costs to the total cost are 64%, 20%, 11%, and 5%, respectively. The cooling water costs are insignificant. The steam requirement is modest because the highly soluble solutes crystallize quite readily and because the temperature difference between the two isotherms T_h and T_c is only 15°C. Clearly, crystallization offers a significant advantage over distillation in energy consumption (Fair, 1987). More details of this cost estimation can be found elsewhere (Dye, 1995).

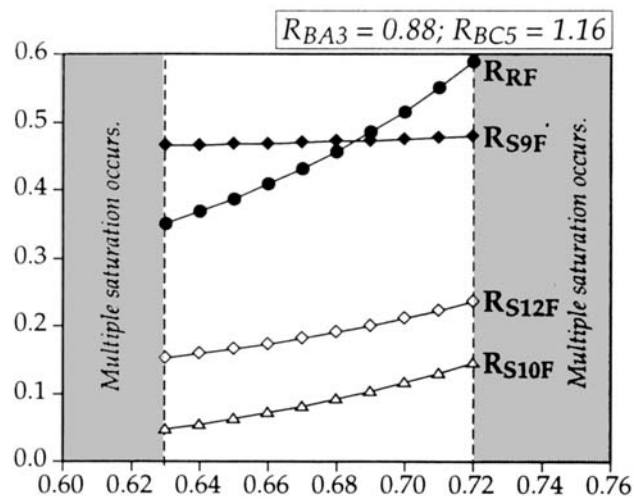

Figure 16. Effect of changes in the ratio R_{BA5}.

Conclusions

Based on the relative positions of the double-saturation points at two different temperatures with respect to the solvent point, a single flowsheet configuration allows complete separation of two-solute mixtures. The three-solute phase behavior, on the other hand, is best characterized by the overlap between region A at one temperature and region C at another, and region C at one temperature and region B at another. If these overlaps exist, it is feasible to separate the three solutes using a new one-loop scheme with two or more isotherms. Otherwise, two-loop schemes are necessary. Two pure solutes, say, A and B, and a eutectic mixture of, say, B and C, are recovered in the first loop. Then, B and C are further separated using one of the two-solute schemes.

A case study of a one-loop, three-solute separation indicates that the cost seems to be quite competitive, although the design variables have not been fully optimized. As mentioned, one can place the operating points such as compositions 2, 4, and 5 in Figure 9b close to the double-saturation troughs so as to increase solute recovery per pass. However, as shown in Figure 15, the recycle flow rate and hence the process cost is very sensitive to the design variable, R_{BA3}. This underscores the need for the designs reported in this article. The operating points should be placed sufficiently far away from the multiple saturation points so that cocrystallization does not occur but the flow rates are not excessive.

It is also clear from the case study that two solute characteristics are highly desirable. For solutes with high solubilities, the amount of solvent to be vaporized can be minimized. For solutes with high freezing points, refrigeration is unnecessary. Additional savings can be realized if heat integration is considered.

The design equations do not provide an exit point for impurities, which are often present in commercial processes. Also, washing and dewatering of the filter cakes have not been considered. Although these considerations are often omitted in conceptual design, more detailed balances are necessary for more realistic process evaluations. The assumption of linear solubility relationships should also be relaxed

to include nonlinear ones in future work. Finally, the design method is based on equilibrium phase diagrams. It is well-known that kinetic effects can significantly influence which species crystallizes. Therefore, while the design method provides a possible flowsheet, experimental testing is crucial to obtain a workable process.

Current practice in the use of fractional crystallization for complete separation is primarily limited to two-solute mixtures. Industrial crystallization of a multicomponent mixture often involves a liquid purge stream. One of the solutes is recovered to the fullest extent possible; the remaining mother liquor is disposed. Clearly, loss of desirable products and excess reactants is an economic concern and the environmental problems related to disposal have become a major issue. For these reasons, fractional crystallization is expected to play a more significant role in separations.

Acknowledgment

Acknowledgment is made to the donors of the Petroleum Research Fund, administered by the ACS, for partial support of this research. Additional support was provided by the National Science Foundation (grant CTS-9220196). We would also like to thank Mr. David A. Berry for his valuable comments, Ms. Pamela Stephan for her graphic artwork, and Professor Frank M. Tiller of the University of Houston for his encouragement to work on fractional crystallization.

Notation

c_i = the concentration of component i (kg i/kg solvent)
$c_i(j)$ = the concentration of component i in stream j (kg i/kg solvent)
F_{iF} = feed flow rate of component i (kg/yr)
R_{RF} = ratio of total flow of recycled solutes and solvent to feed flow
S_i''' = triple-saturation joint solubility of component i (kg i/kg solvent)

Literature Cited

Cisternas, L. A., and D. F. Rudd, "Process Designs for Fractional Crystallization from Solution," *Ind. Eng. Chem. Res.*, **32**, 1993 (1993).

Dale, G. H., "Crystallization, Extractive and Adductive," *Encycl. Chem. Process. Des.*, **13**, 456 (1981).

Dye, S. R., "Crystallization-Based Separation Processes," PhD Diss., Dept. of Chemical Engineering, Univ. of Massachusetts, Amherst (1995).

Dye, S. R., and K. M. Ng, "Bypassing Eutectics with Extractive Crystallization: Design Alternatives and Tradeoffs," *AIChE J.*, **41**, 1456 (1995).

Dye, S. R., D. A. Berry, and K. M. Ng, "Synthesis of Crystallization-Based Separation Schemes," *Proc. Found. Computer-Aided Proc. Des., AIChE Symp. Ser.*, **91**, 238 (1995).

Fair, J. R., "Energy-Efficient Separation Process Design," in *Recent Developments in Chemical Process and Plant Design*, Y. A. Liu, H. A. McGee, Jr., and W. R. Epperly, eds., Wiley, New York (1987).

Fischer, O., S. J. Jancic, and K. Saxer, "Purification of Compounds Forming Eutectics and Solid Solutions by Fractional Crystallization," in *Industrial Crystallization*, S. J. Jancic and E. J. de Jong, eds., Elsevier Science, New York, p. 153 (1984).

Fitch, B., "How to Design Fractional Crystallization Processes," *Ind. Eng. Chem.*, **62**(12), 6 (1970).

Gilbert, S. W., "Melt Crystallization: Process Analysis and Optimization," *AIChE J.*, **37**, 1205 (1991).

Mullin, J. W., *Crystallization*, 3rd ed., Butterworth-Heinemann, Oxford (1993).

Myerson, A. S., ed., *Handbook of Industrial Crystallization*, Butterworth-Heinemann, Boston (1993).

Ng, K. M., "Systematic Separation of a Multicomponent Mixture of Solids Based on Selective Crystallization and Dissolution," *Sep. Tech.*, **1**, 108 (1991).

Nishida, N., G. Stephanopoulos, and A. W. Westerberg, "A Review of Process Synthesis," *AIChE J.*, **27**, 321 (1981).

Rajagopal, S., K. M. Ng, and J. M. Douglas, "Design of Solids Processes: Production of Potash," *Ind. Eng. Chem. Res.*, **27**, 2071 (1988).

Rajagopal, S., K. M. Ng, and J. M. Douglas, "Design and Economic Trade-Offs of Extractive Crystallization Processes," *AIChE J.*, **37**, 437 (1991).

Rousseau, R. W., ed., *Handbook of Separation Process Technology*, Wiley, New York (1987).

Sciance, C. T., and L. S. Scott, "Process for Separation of Glutaric, Succinic and Adipic Acids," U. S. Patent, 3,338,959 (1967).

Manuscript received Aug. 25, 1994, and revision received Dec. 9, 1994.